ChemBioChem

Supporting Information

Multimodal Molecular Imaging and Identification of Bacterial Toxins Causing Mushroom Soft Rot and Cavity Disease

Benjamin Dose[+], Tawatchai Thongkongkaew[+], David Zopf[+], Hak Joong Kim, Evgeni V. Bratovanov, María García-Altares, Kirstin Scherlach, Jana Kumpfmüller, Claudia Ross, Ron Hermenau, Sarah Niehs, Anja Silge, Julian Hniopek, Michael Schmitt, Jürgen Popp,* and Christian Hertweck*

Table of Contents

Figures

Tables

Experimental Section

1. Bacterial strains and cultivation conditions

For this study *Burkholderia gladioli* pv. *agaricicola* HKI0676 was cultured in potato dextrose broth (PDB; BD, Bacto®) at 30 °C and 110 rpm or on PDA (15 g mL^{-1} agar added to PDB). Further media for culturing were: malt extract agar (20 g L^{-1} malt extract (BD, Bacto®); 1 g L^{-1} peptone (BD, Bacto®), 20 g L^{-1} D-glucose, 15 g L^{-1} agar in dH_2O), chicken soup powder media (CSP-M) (5 g L^{-1} chicken soup powder trademark "LOBO", ingredients: salt, sugar, spices (onion powder, white pepper powder, garlic powder), flavor enhancer: E621, chicken powder (chicken, salt, onion, wheat, soybean), dextrose, anti-caking agent: E551; 2 g L^{-1} sucrose (BD, Bacto®) dH_2O) or in MGY (1.25 g L^{-1} yeast extract (BD, Bacto®), 10 g L^{-1} glycerol, M9 salts: 50 × part A: 350 g L^{-1} K_2PO_4, 100 g L^{-1} KH_2PO_4, 50 × part B: 29.4 g L^{-1} Tri-Na-citrate-dihydrate, 50 g L^{-1} $(NH_4)_2SO_4$, 5 g L^{-1} $MgSO_4$,). *E. coli* strains were cultured in LB medium (10 g L^{-1} tryptone (BD, Bacto®), 5 g L^{-1} yeast extract (BD, Bacto®), 10 g L^{-1} NaCl; for agar: addition of 1.5 % agar) or on LB agar plates at 37 °C with appropriate antibiotic concentrations (kanamycin 50 µg mL^{-1}, apramycin 50 µg mL^{-1}). For long-time storage bacterial strains were stored in 25 % glycerol at –20 °C.

Table S1. Bacterial strains used in this study.

Strain	No.	Original site of isolation or supplier
Burkholderia gladioli pv. *agaricicola*	HKI0676	Rotten *Agaricus bisporus*
Escherichia coli	TOP10	ThermoFisher Scientific
Escherichia coli	XL1-Blue	Agilent Technologies

2. Metabolic profiling

Fresh mushrooms were washed twice with cold water to remove dirt. The mushrooms were cut in a laminar flow cabinet and placed in petri dishes. The sliced mushrooms were inoculated with a suspension of an overnight culture of *B. gladioli* pv. *agaricicola* HKI0676 and then incubated at 30 °C. When the lesions became visible after 16 h of cultivation, the infected mushrooms were extracted with ethyl acetate. Crude extracts were analyzed by LC-HRESI-MS. Compounds were identified based on their UV spectra and high-resolution mass by comparison with authentic references. The same procedure was repeated for non-infected mushrooms and with sterile respective media as a negative control. Alternatively, *B. gladioli* pv. *agaricicola* HKI0676 cultures were incubated for 4 days at 30 °C on malt extract agar, in CSP-M or on MGY agar. Again, sterile agar or media (MEA, CSP-M and MGY) were treated in parallel and extracted as described before. All culturing conditions were replicated with the knockout strains.

3. Analytical HR-ESI-LC/MS

High-resolution mass spectrometry measurements were performed on an Exactive Orbitrap High Performance Benchtop LC-MS (Thermo Fisher Scientific) with an electron spray ion source and an Accela HPLC System, C18 column (Betasil C18, 150 × 2.1 mm, Thermo Fisher Scientific). As solvents acetonitrile and distilled water (both supplemented with 0.1% formic acid) were used with a flow rate of 0.2 mL min^{-1} and the following program: hold 1 min at 5 % acetonitrile, 1–16 min 5–98 % acetonitrile, hold 3 min 98 % acetonitrile, 19–20 min 98 % to 5 % acetonitrile, and hold 3 min at 5 % acetonitrile. Detected Metabolites are listed down below:

3.1. Haereogladin A (1)

HRESI-MS: *m/z* = 859.3890 $[M+H]^+$ calculated for $C_{44}H_{55}N_6O_{12}$ *m/z* = 859.3872

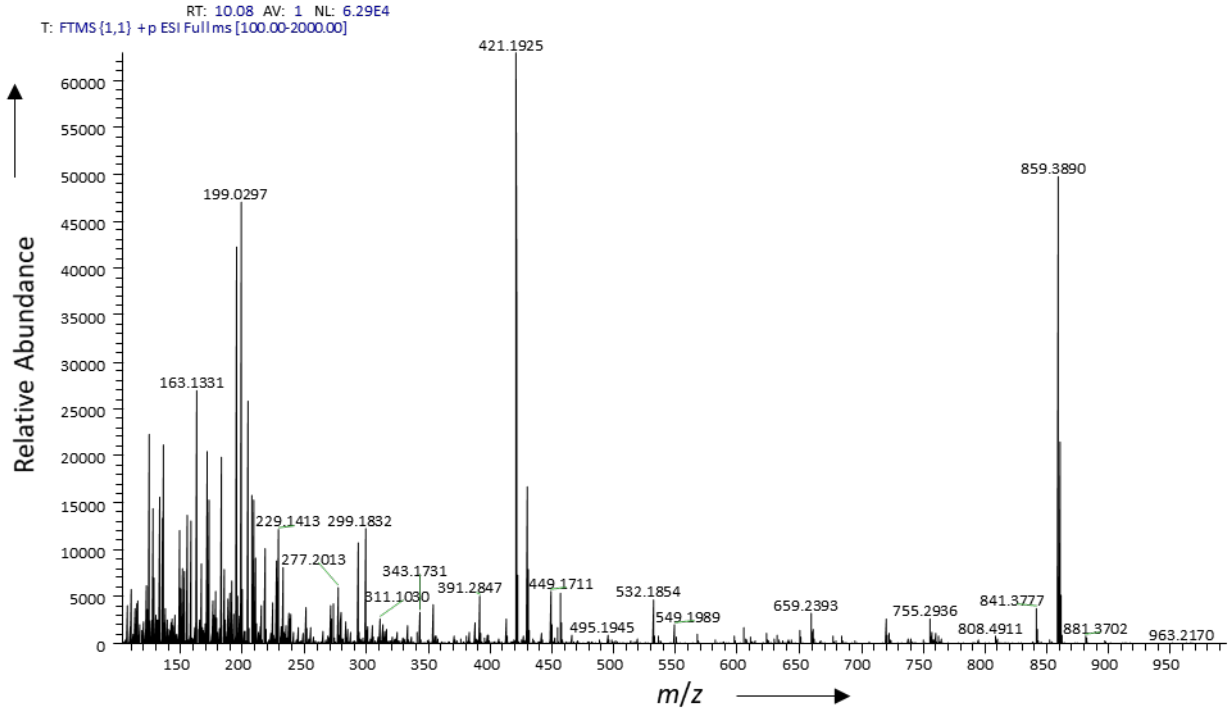

Figure S1. HRESI-MS spectrum of haereogladin A (**1**).

3.2. Burriogladin A (2)

HRESI-MS: *m/z* = 961.5034 $[M+H]^+$, calculated for *m/z* = $C_{49}H_{69}N_8O_{12}$ 961.5029

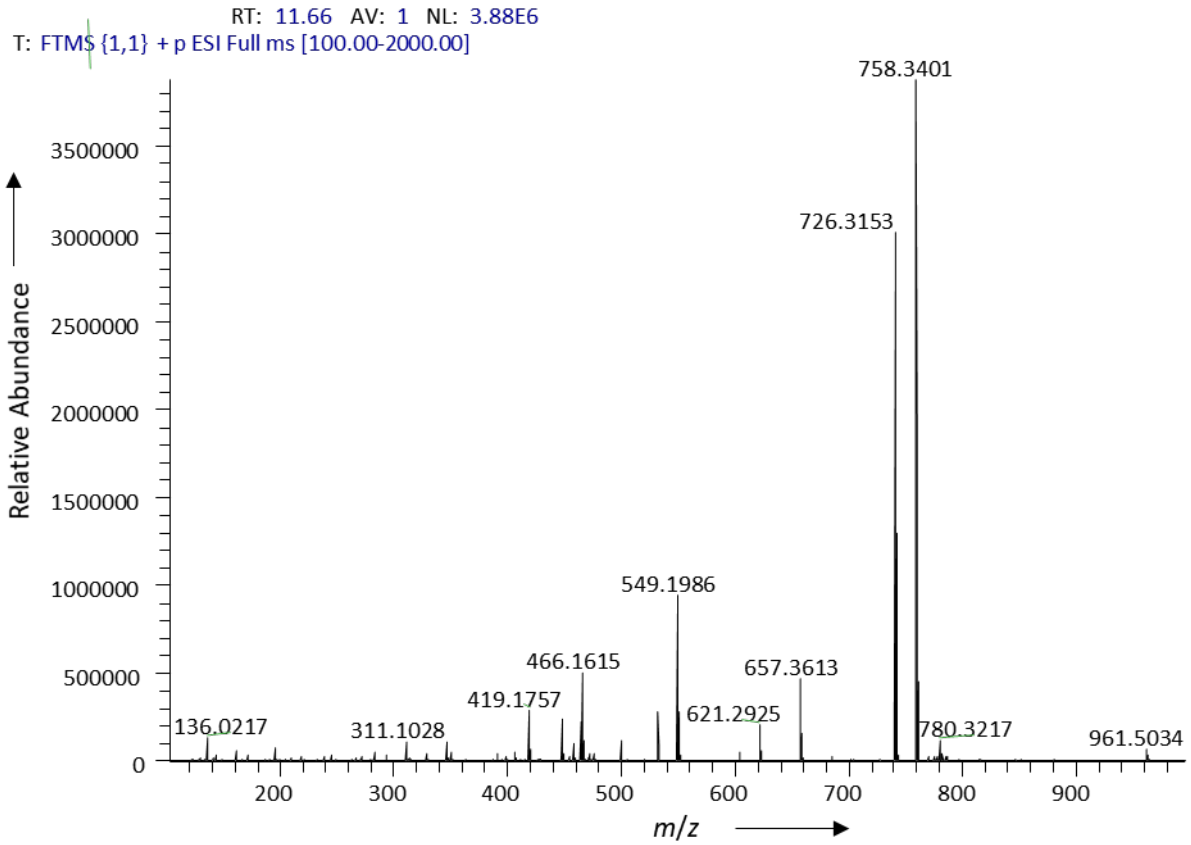

Figure S2. HRESI-MS spectrum of burriogladin A (**2**).

3.3. Icosalide A1 (4)

HRESI-MS: *m/z* = 711.4559 $[M-H]^-$, calculated for $C_{36}H_{63}N_4O_{10}$ *m/z* = 711.4550

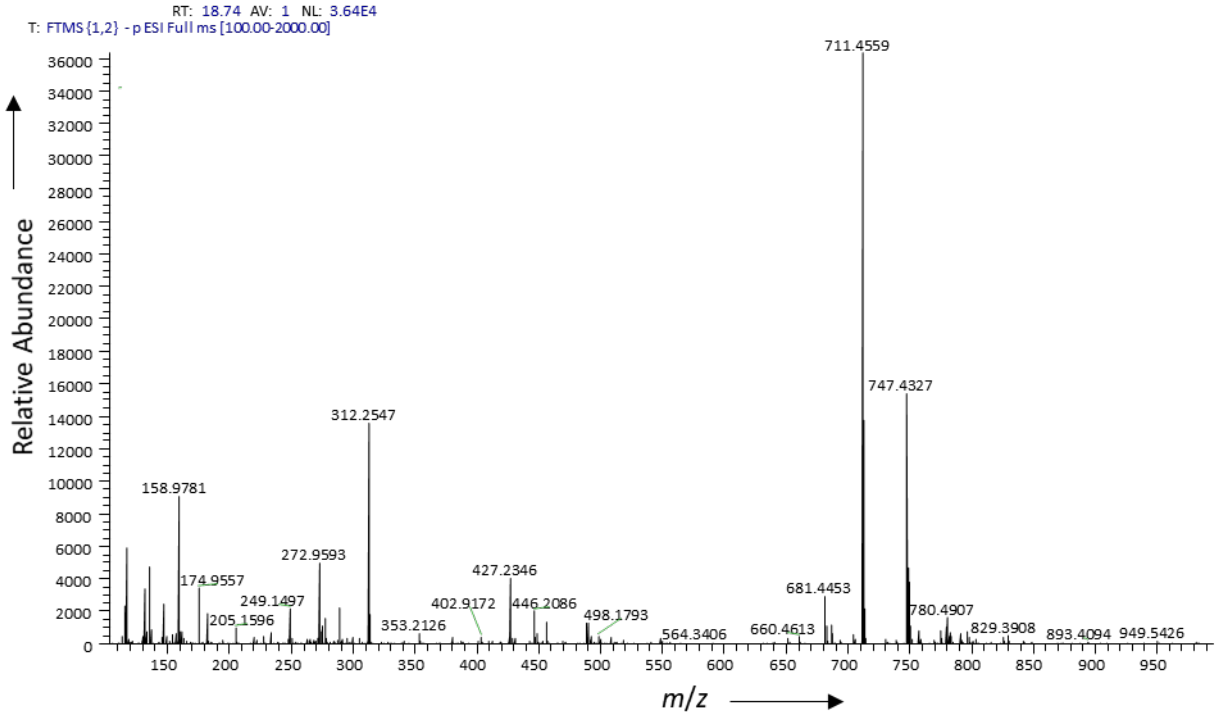

Figure S3. HRESI-MS spectrum of icosalide A1 (**4**).

3.4. Gladiofungin A (5)

HRESI-MS: *m/z* = 504.2607 $[M-H]^-$, calculated for $C_{27}H_{38}NO_8$ *m/z* = 504.2603

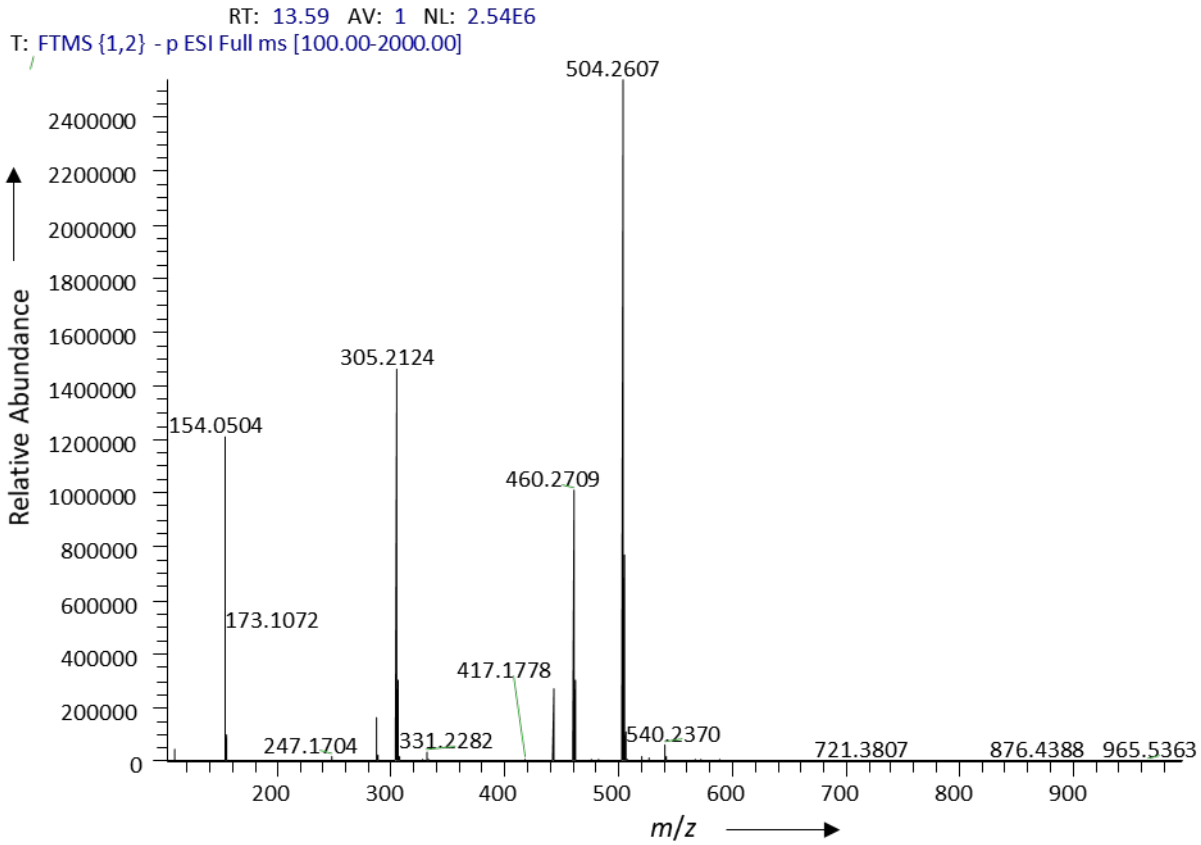

Figure S4. HRESI-MS spectrum of gladiofungin A (**5**).

3.5. Enacyloxin IIa (6)

HRESI-MS: *m/z* = 700.2311 $[M-H]^-$, calculated for $C_{33}H_{44}NO_{11}Cl_2$ 700.2297

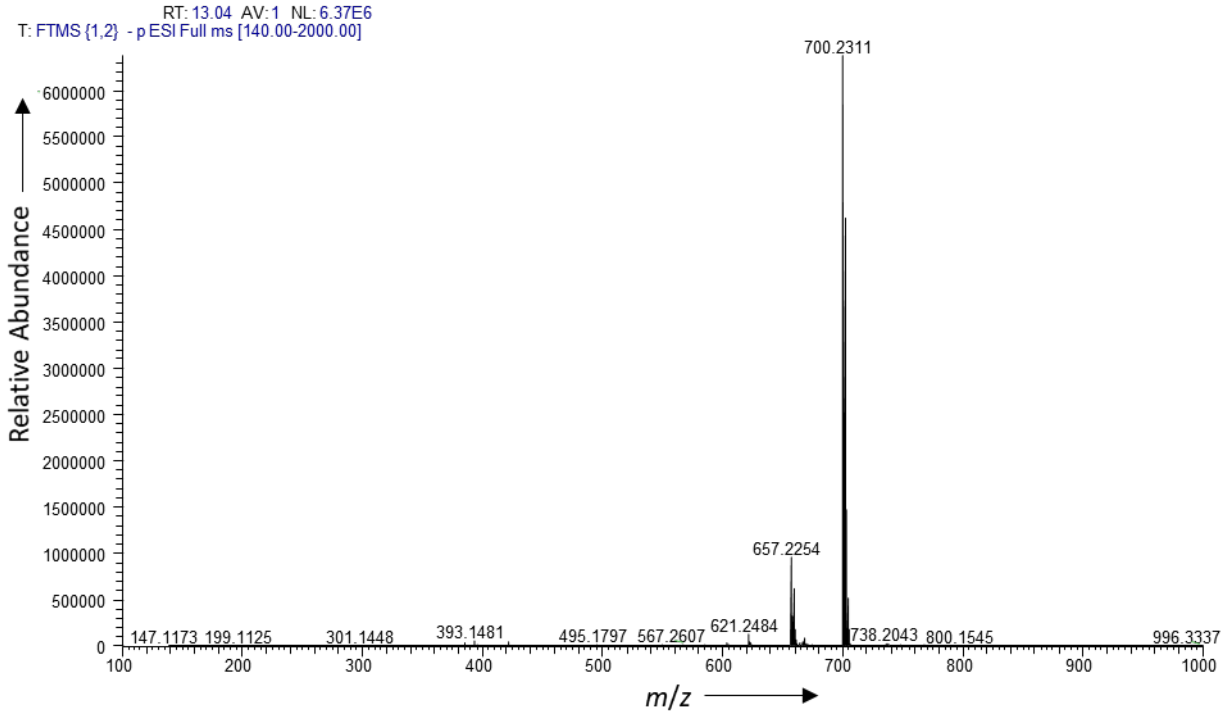

Figure S5. HRESI-MS spectrum of enacyloxin IIa (**6**).

3.6. Caryoynencin (7)

HRESI-MS: *m/z* = 279.1029 $[M-H]^-$, calculated for $C_{18}H_{15}O_3$ *m/z* = 279.1021

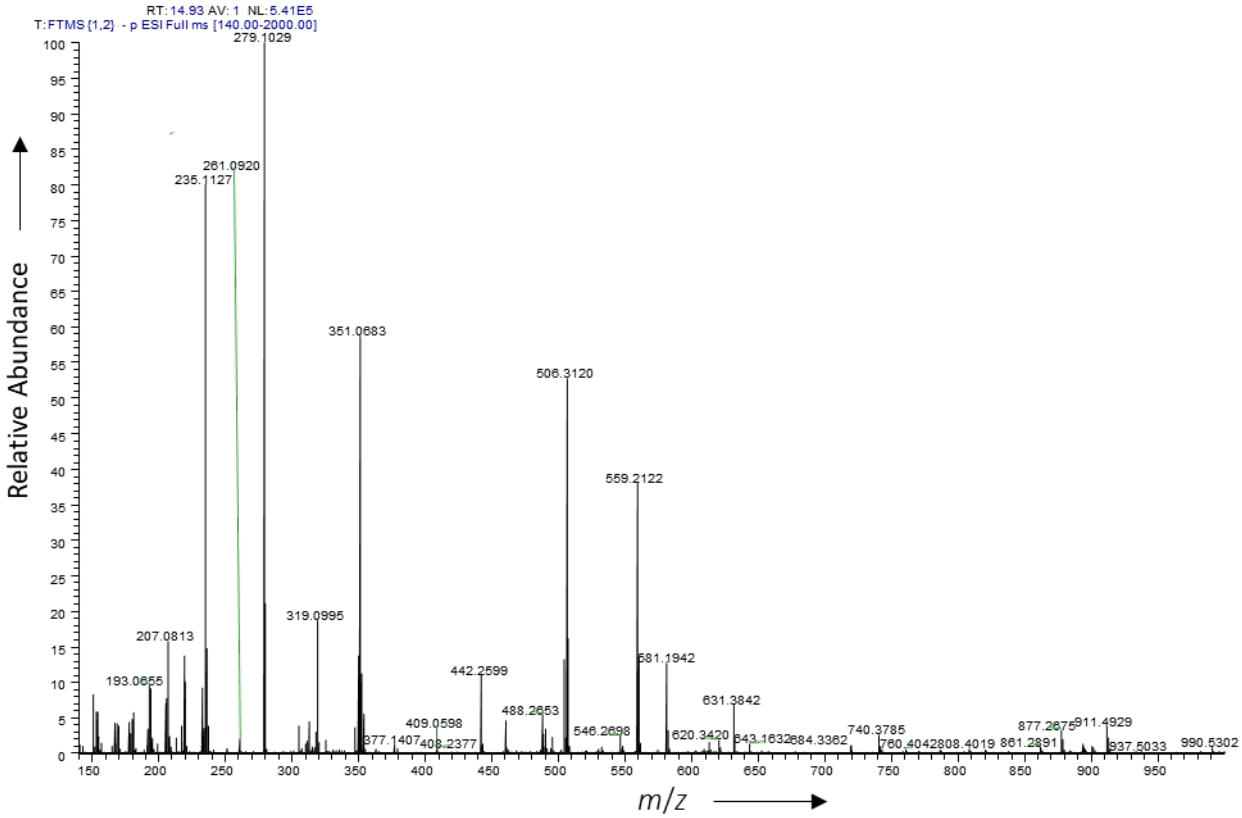

Figure S6. HRESI-MS spectrum of caryoynencin (**7**).

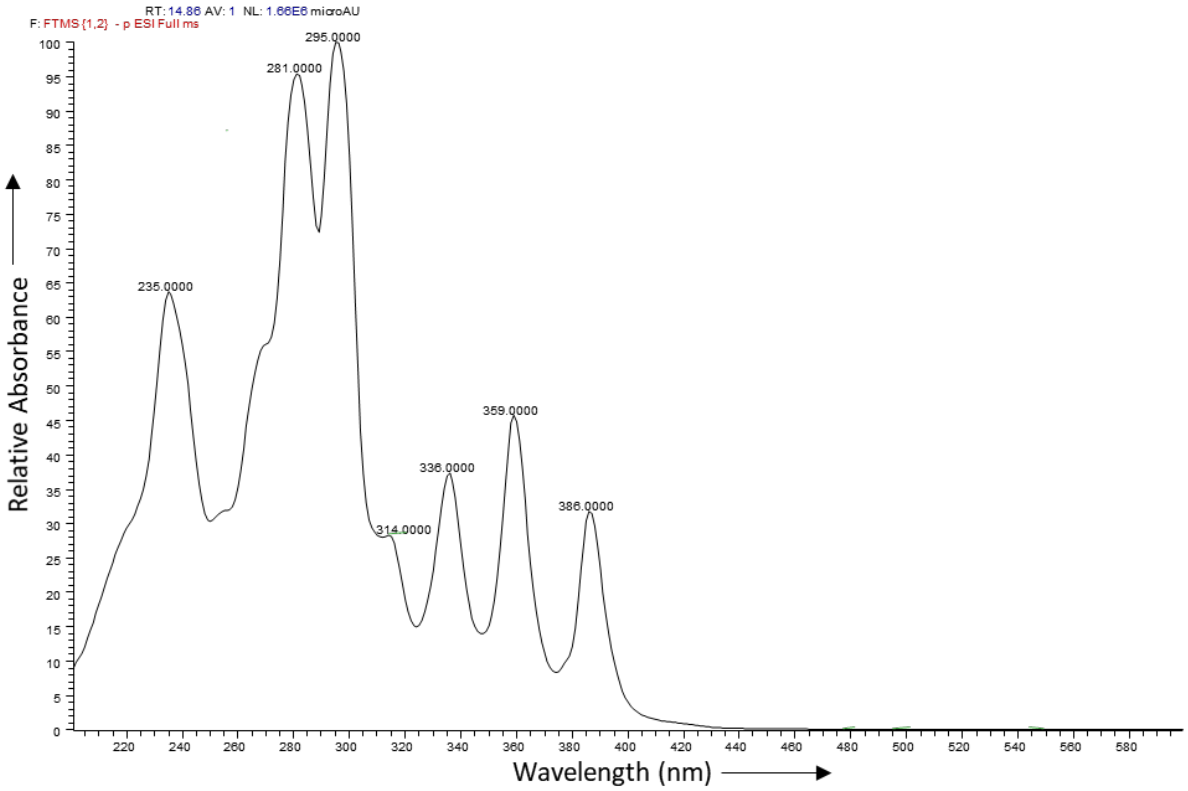

Figure S7. UV spectrum of caryoynencin (**7**) (PDA).

3.7. Sinapigladioside (8)

HRESI-MS: *m/z* = 468.1341 $[M-H]^-$, calculated for $C_{21}H_{26}NO_9S$ *m/z* = 468.1334

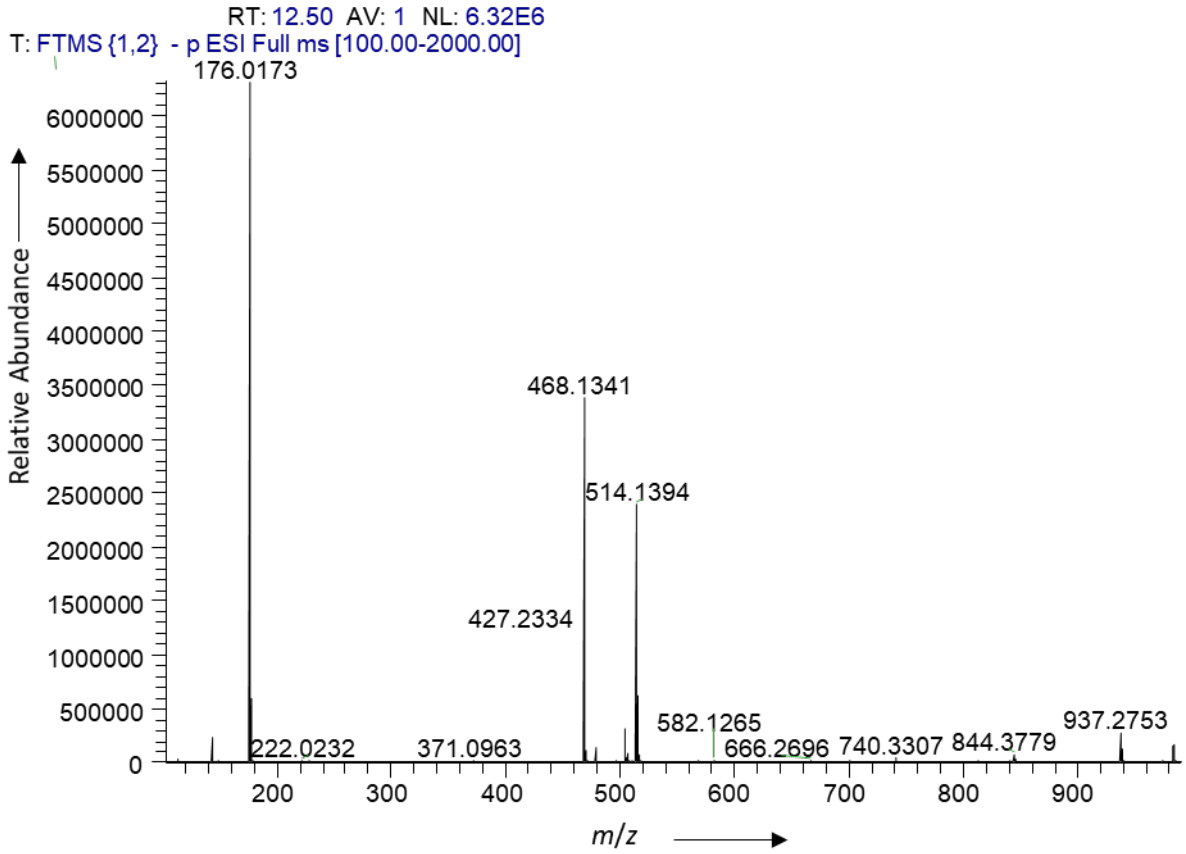

Figure S8. HRESI-MS spectrum of sinapigladioside (**8**).

3.8. Toxoflavin (9)

HRESI-MS: *m/z* = 194.0672 $[M+H]^+$, calculated for *m/z* = $C_7H_8N_5O_2$ 194.0673

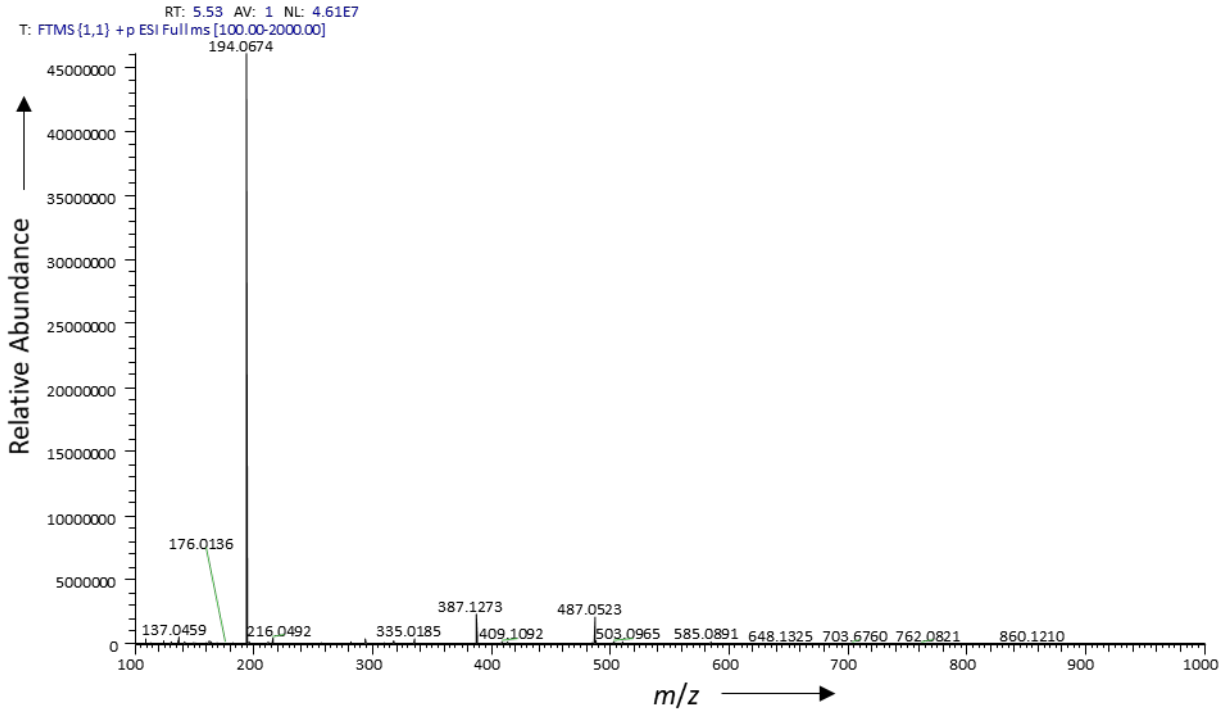

Figure S9. HRESI-MS spectrum of toxoflavin (**9**).

4. 16S RNA Phylogenetic analysis

A maximum likelihood phylogenetic tree was constructed based on 16S rRNA genes of ecologically diverse members of the genus *Burkholderia* as described previously.[1] NCBI accession numbers: NC_010682.1 *Ralstonia pickettii* 12J; CP009322.1 *Burkholderia gladioli* strain ATCC 10248; NC_015381.1 *Burkholderia gladioli* BSR3; KN151012.1 *Burkholderia gladioli* UCD-UG_CHAPALOTE; NZ_CP007212.1 *Burkholderia plantarii* strain ATCC 43733; NZ_CP002581.1 *Burkholderia glumae* PG1; NR_042393.1 *Burkholderia rhizoxinica* strain HKI 454; NR_027587.1 *Burkholderia thailandensis* strain E264; NR_116142.1 *Burkholderia* endo*fungorum* strain CIP 107096; NR_118064.1 *Burkholderia graminis* strain C4D1M; NR_074299.2 *Burkholderia mallei* strain ATCC 23344; NR_043553.1 *Burkholderia pseudomallei* strain ATCC 23343; NR_114491.1 *Burkholderia cepacia* strain ATCC 25416; *Burkholderia gladioli* pv. *agaricicola*. The tree was rooted using 16S rRNA gene of NR_043152 *Ralstonia picketii* 12J.BGC encoded in the respective *Burkholderia* genomes were manually identified by sequence comparisons to known biosynthesis genes.

5. Generation of null mutants of *B. gladioli* pv. *agaricicola* HKI0676

Target genes were inactivated by insertion of a resistance cassette as the result of homologous recombination with a plasmid. Mutants for gene inactivation of key genes in the biosynthesis of toxoflavin (**9**) (*B. gladioli* pv. *agaricicola* HKI0676 Δ*tox*), sinapigladioside (**8**) (*B. gladioli* pv. *agaricicola* HKI0676 Δ*spg*), caryoynencin (**7**) (*B. gladioli* pv. *agaricicola* HKI0676 Δ*cay*), gladiofungin (**5**) (*B. gladioli* pv. *agaricicola* HKI0676 Δ*gla*) and icosalide (**4**) (*B. gladioli* pv. *agaricicola* HKI0676 Δ*ico*) were detected by colony PCRs. *B. gladioli* cells were transformed with knockout plasmids to inactivate genes of interest as described in previous studies.[2] The transformants were plated on NAG plates with 300 µg mL^{-1} kanamycin respectively apramycin and incubated at 30 °C until colonies appeared. Since the recombination integrates a resistance cassette into the genome of the transformants, mutated clones can be selected for on appropriate antibiotics and detected by colony PCRs.

5.1. Caryoynencin BGC knockout plasmid

The *cayC* gene in the biosynthetic gene cluster of caryoynencin (**7**) was amplified using the primers cayC FI1 and cayC FI2 (Table S2) from the genomic DNA from *B. caryophylli* using Phusion High-Fidelity DNA Polymerase with 5 % DMSO (New England Biolabs, Frankfurt am Main, Germany) and (98 °C for 3 min; 35 cycles: 98 °C for 15 s, 65 °C for 15 s and 72 °C 1 min kb^{-1}) according to the manufacturers recommendations. Ligation with an apramycin resistance gene cassette amplified from pIJ773[3] using the primers AprR-fwd and AprR-rv yielded a combined gene fragment that was ligated with pJET1.2/blunt vector and transferred into *E. coli* XL1-Blue cells. The vector named pHK102 containing the combined gene fragment was purified and partially sequenced. Due to the high degree of sequence similarity between the *cayC* gene from *B. caryophylli* and the homologous gene from *B. gladioli* pv. *agaricicola,* the gene inactivation plasmid can be used to inactivate the homologues of *cayC* in both strains.

5.2. Sinapigladioside BGC knockout plasmid

The *isnA* sinapigladioside biosynthesis gene[4] was amplified by PCR from the genomic DNA of *B. gladioli* using the primers BD115 and BD116 as well as BD119 and BD120. The kanamycin resistance cassette was generated by PCR using the primers BD117 and BD118 and pGEM-Kan[5] as a template. The PCRs were performed using Phusion High-Fidelity DNA Polymerase with 5 % DMSO (New England Biolabs, Frankfurt am Main, Germany) and (98 °C for 3 min; 35 cycles: 98 °C for 15 s, 65 °C for 15 s and 72 °C 1 min kb^{-1}). The three PCR products were subjected to a NEBuilder reaction according to the manufacture's recommendations. The NEBuilder mix was subsequently blunt-end ligated into pJET1.2 yielding pBD43 (Table S3).

5.3. Toxoflavin BGC knockout plasmid

The toxoflavin BGC cluster (*tox*) was reported in *B. glumae*[6] and *B. gladioli*,[7] yet the gene cluster could not be detected within the available genome sequence of *B. gladioli* pv. *agaricicola*. Due to the high degree of sequence similarity between these strains, a gene inactivation plasmid was constructed using the toxoflavin gene cluster in *B. gladioli* as template. Primers were designed to amplify the sequences of *tox*C (ABQ88344.1) and *toxD* (ABQ88345.1) using genomic DNA of *B. glumae* as a template. "Flanking region 1" and "Flanking region 2" were amplified using Kapa HiFi DNA polymerase (Kapa Biosystems) following the manufacturer's recommendations in a two-step nested PCR from gDNA of *B. gladioli* pv. *agaricicola.* The outer primers for the initial PCR were ToxKO_NEB_FL1_F and ToxKO_NEB_FL2_R. The following PCR conditions were used: (95 °C for 3 min, 30 cycles of 95 °C for 15 s, 60 °C for 15 s, 72 °C for 30 s kb^{-1} and final step at 72 °C for 10 min. The obtained amplicon (~ 2,400 bp) was gel purified and used as a template for a second PCR using ToxKO_NEB_FL1_F and ToxKO_NEB_FL1_R (for "Flanking region 1") and ToxKO_NEB_FL2_F and ToxKO_NEB_FL2_R (for "Flanking region 2"). In addition, a kanamycin resistance cassette was amplified using pGEM-Kan[5] as a template, Kan_2_ToxKO_NEB_F and Kan_TaxKO_NEB_R and Kapa HiFi DNA polymerase. The obtained DNA fragments "Flanking region 1", the kanamycin resistance cassette and "Flanking region 2" were fused together using NEBuilder® HiFi DNA Assembly Master Mix (New England Biolabs) following the manufacturer's recommendations. Subsequent ligation into pJET1.2 (Thermo Fischer Scientific) yielded pEB70. A list of constructed plasmids can be found in Table S3.

5.4. Icosalide and gladiofungin BGC knockout plasmids

The knockout plasmids targeting the icosalide (pBD58) and gladiofungin (pJK345) biosynthesis genes were taken from previous studies.[2, 8]

Table S2. Primers used in this study.

Gene or name	Sequence (5' → 3')
AprR-fwd	gctacgctagcattccggggatccgtcgacc
AprR-rv	gctacttaattaatgtaggctggagctgcttc
*cay*C Fl1-fwd	acgtatcaaggcgttgaccgc
*cay*C Fl1-rv	gctacttaattaagctagcgtagcacccagaatagaatcggac
*cay*C Fl2-fwd	gctacgctagcttaattaagtagcattgccaatcagttcgcg
*cay*C Fl2-rv	gacgcggtcgatcatgt
BD115	ctgaagcgggctcattcgacgc
BD116	actgttgcaaatagtagcgcgcgatccgcgctg
BD117	cgcggatcgcgcgctactatttgcaacagtgccgttg
BD118	cctgcaccagcggattcagccaatcgactggcg
BD119	cagtcgattggctgaatccgctggtgcaggaggac
BD120	gcctgggcacgaacggcag
BD158	gatcggcatcaccattcc
BD159	gaaccgagcgagacgtagac
BD158	gatcggcatcaccattcc
BD159	gaaccgagcgagacgtagac
Apra_seq_fw	ggagctgtggaccagcagc
Apra_seq_rv	ctcgagaatgaccactgc
ToxKO_NEB_FL1_F	cttcctcgtccgactacacc
ToxKO_NEB_FL1_R	ctgatcgaggcgaagtagc
Kan_2_ToxKO_NEB_F	gcgagggctacttcgcctcgatcaggtaagcttaggctgctgcca
Kan_TaxKO_NEB_R	tgtcagccaacttgatggtctcagaagaactcgtcaagaag
ToxKO_NEB_FL2_F	gaccatcaagttggctgaca
ToxKO_NEB_FL2_R	ccgggataggcacgatagtc
ToxKO_chk_F	cgcgaccagtacgtgctgac
ToxKO_chk_R	gctacctgctttctctttgcgct

Table S3. Plasmids used in this study.

Plasmid name	Resistance	Generation of *B. gladioli* pv. *agaricicola* strains
pHK102	apramycin, ampicillin	Δ*cay*
pEB70	kanamycin	Δ*tox*
pBD43[4]	apramycin, ampicillin	Δ*spg*
pBD58[2]	kanamycin	Δ*ico*
pJK345[8]	kanamycin	Δ*gla*

5.5. PCR-based mutant detection

Transformed cells were screened for mutants using colony PCRs. The Δ*cay* mutant strain was verified by colony PCR using primers cayC Fl1-fwd and cayC Fl2-rv, colony material, a master mix of KAPA2G Robust HotStart ReadyMix PCR kit (Merck KGaA, Darmstadt), 3% DMSO and 95 °C for 3 min and 35 cycles of 95 °C for 30 s, 60 °C for 30 s kb^{-1}, and a final extension time at 72 °C for 300 s. Mutants yield a 1,934 bp and wildtype strains a 960 bp PCR fragment. The lack of caryoynencin (**7**) production can be further visualized on PDA agar plates as Δ*cay* mutants lack the characteristic, brown-colored colony phenotype (Figure S10).

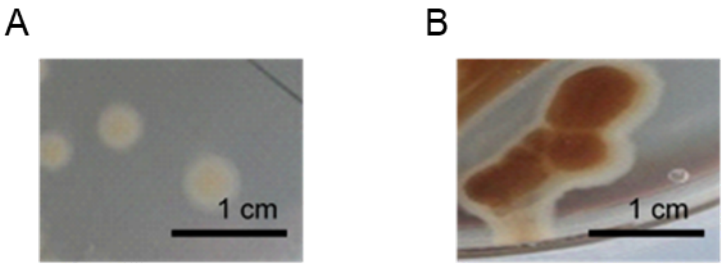

Figure S10. Pictures of A) *B. gladioli* pv. *agaricicola* Δ*cay* and B) wild type colonies grown on PDA for 2–3 weeks.

A *B. gladioli* pv. *agaricicola* HKI0676 Δ*spg* mutant was identified by colony PCR using the same conditions as stated for Δ*cay* mutants. Colony PCRs using the indicated primer pairs yielded a 1,410 bp fragment (BD158 and Apra_seq_fw) as well as a 1,508 bp fragment (BD159 and Apra_seq_rv), indicating inactivation of the target gene. A *B. gladioli* pv. *agaricicola* HKI0676 Δ*tox* knockout strain was identified by colony PCR using ToxKO_chk_F and ToxKO_chk_R yielding a 1,529 bp product for the mutant. Sequencing of the purified products verified the insertion of the resistance cassettes in all generated mutant strains. Knockout mutant strains were incubated for 4 days at 30 °C on malt extract agar, in CSP-M or on MGY agar to produce sinapigladioside (**8**), caryoynencin (**7**) or toxoflavin (**9**), respectively. LC-ESI-HRMS measurements of the extracts confirmed the successful mutations, as the respective natural product could not be detected.

6. Mycelium growth assay

Malt extract agar was melted in a microwave and the temperature of the molten agar was adjusted to 50 °C in a water bath. Next, 10 mL of the molten agar were transferred onto a sterile petri dish (94 × 16 mm). Then, 40 µL of 2,500 µg mL^{-1} toxin solution in DMSO were mixed with the molten agar in petri dish. The final concentration of the toxin in the agar is 10 µg mL^{-1}. The toxin-containing agar was dried under a laminar flow cabinet for 30 min. After the agar was solidified, a 30-day old culture of *A. bisporus* mycelium was placed at the center of the toxin-containing agar plate and incubated at room temperature.

After 20 days, photos of mycelium were taken from the backside of the petri dish and the area covered by mycelium measured. The area of mushroom mycelium growth obtained from the same photo was independently calculated three times (Table S4). The area from the same photo is considered as a technical replicate. Three values of area from the same photo were averaged and a mean value was reported. This experiment was repeated in nine biological replicates. For data visualization, fifteen values of means from fifteen biological replicates were represented using box plot. For statistical analysis, the normality of data was evaluated by the Shapiro-Wilk test. Since the data is not normally distributed, the Mann-Whitney *U* test was used for statistical analysis. *p*-value lower than 0.05 is considered as statistically different.

Table S4. Testing the effects of different additives on the mycelium growth of *A. bisporus* on PDA agar plates. Final concentration of additives after mixing with agar is 10 µg mL^{-1} DMSO = negative control, tebuconazole = positive control.

Biol. replicate	Area of mycelium growth (cm^2), average from three technical replicates						
	No additive	DMSO	Tebuconazole	Toxoflavin (9)	Sinapigladioside (8)	Crude extract (7)	PDB extract
1	20.36	23.35	4.21	18.67	1.80	14.19	19.92
2	20.69	19.62	3.23	18.66	10.14	16.86	21.37
3	21.45	19.74	3.08	20.50	2.45	16.35	22.36
4	25.65	24.98	4.42	19.68	2.27	15.27	20.23
5	26.29	27.67	3.61	19.92	8.64	15.74	19.89
6	25.76	26.23	4.92	18.50	2.72	15.28	19.88
7	20.17	18.66	3.46	15.05	2.55	16.60	19.73
8	19.60	20.28	7.43	12.66	6.01	15.29	20.30
9	20.82	17.13	4.18	15.87	3.35	16.16	19.13

7. Biological assays using mushroom slices

Spotting of solvents (20 µL) that are frequently used to dissolve secondary metabolites for biological testing (Figure S11a). To test the effects of gene knockout strains on mushroom slices, we infected mushroom slices with the null producer strains of *B. gladioli* pv. *agaricicola* (Δ*spg*, Δ*tox*, Δ*ico*, Δ*gla*, Δ*cay*) and wild type. Samples were inoculated with 20 µL of an overnight bacteria culture and incubation at 30 °C for up to three days (Figure S11b).

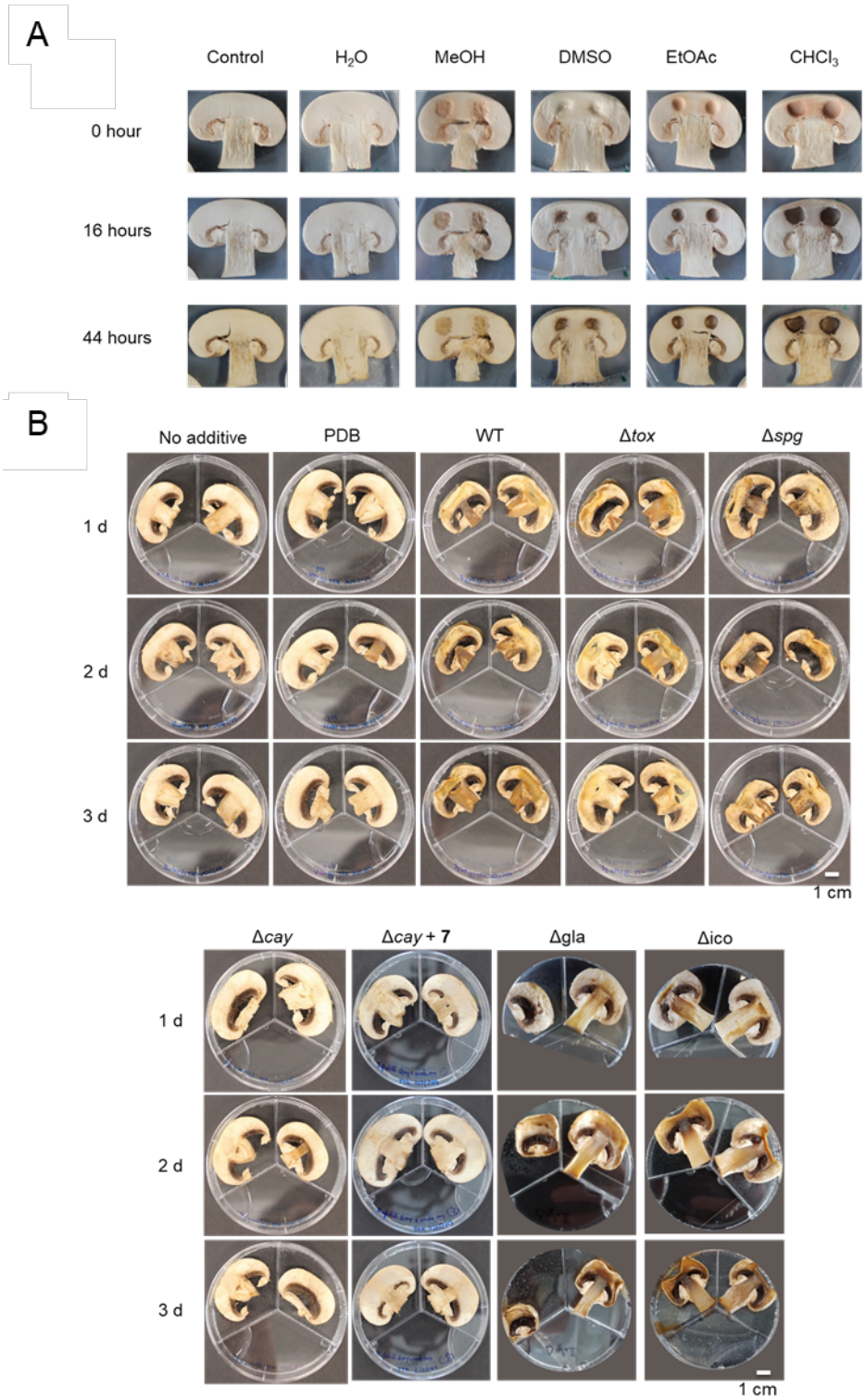

Figure S11. Testing of organic solvents, null producer strains or wild type (WT) of *B. gladioli* pv. *agaricicola* on mushroom slices. A) Spotting of organic solvents and water on mushroom slices. H_2O, Wasser; MeOH, Methanol; Dimethyl sulfoxide; EtOAc, Ethyl acetate; $CHCl_3$, Chloroform. B) Infection assay of mushroom slices with *B. gladioli* pv. *agaricicola* wild type and indicated knockout strains as well as a Δ*cay* complemented with 5 µL (2 µg $µL^{-1}$) **7** crude extract, incubated at 30 °C for up to three days.

8. MALDI imaging

Sliced mushroom (< 0.5 mm) was placed on a conductive tape attached to an ITO-coated glass slide for MALDI imaging mass spectrometry. The sliced mushroom was inoculated with a single colony from an overnight culture of *B. gladioli* pv. *agaricicola* HKI0676 grown on PDA at 30 °C. The bacterial cells were spread throughout the mushroom surface using an inoculation loop. Next, the infected mushrooms were cultivated at 30 °C. After 16 h, the infected mushroom was dried in an incubator at 30 °C overnight. A dried sample of infected mushroom was sprayed twice with a solution of MALDI universal matrix in CH_3CN (4 mL of a 7 mg mL^{-1} solution, matrix composition: 1 : 1 mixture of 2,5-dihydroxybenzoic acid and α-cyano-4-hydroxycinnamic acid, Sigma Aldrich). An ImagePrep device 2.0 (Bruker Daltonics) was used to spray the matrix solution. Before the MALDI imaging measurement, the sample coated with matrix was dried again in an incubator at 30 °C, overnight (Figure S12a). The mass spectra were recorded from *m/z* 0 to 2,000 in positive ionization mode. The whole mushroom slice, including infected tissues in the middle and non-infected tissues (the rest), indicated with a red line in Figure S12b was measured. In total, 10,274 mass spectra were analyzed and visualized by FlexImaging software (Bruker).

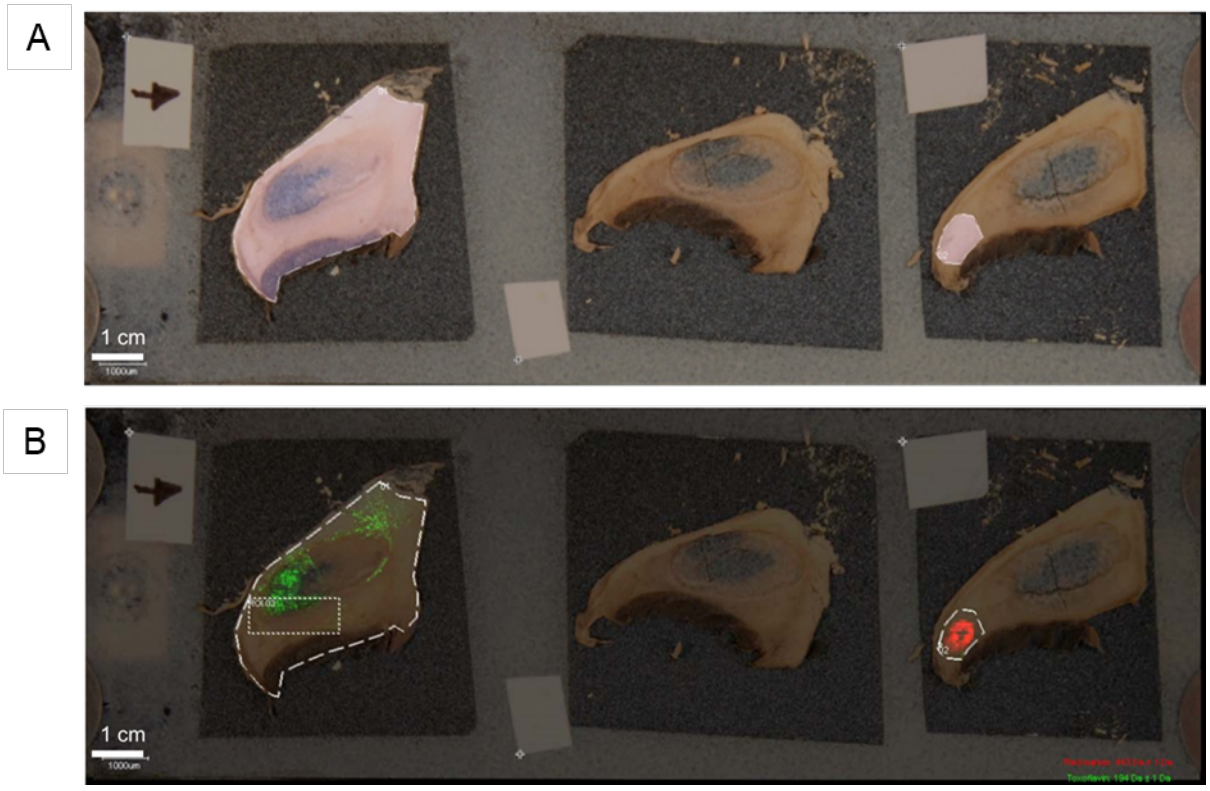

Figure S12. MALDI imaging of infected mushroom slices. A) Infected mushrooms (triplicate), dried with matrix. B) MALDI imaging of infected mushroom tissue, visualization of *m/z* 194 $[M+H]^+$ and a red marker as reference (443 *m/z* $[M+H]^+$).

9. Raman investigation

The UV Raman spectra of dissolved extracts and mushroom slices were recorded using a Raman microscope (HR800, Horiba/Jobin-Yvon). The excitation light of 244 nm was generated with an intracavity frequency-doubled line of an argon ion laser (Innova 300, FRED, Coherent Inc., Santa Clara, CA, USA; power measured at the laser output ~ 15 mW). The focus point on the sample was adjusted with a 15 × anti-reflection coated objective (LMU UVB). The Raman-scattered light was directed through an entrance slit (width = 300 µm) towards a diffraction grating (2,400 lines mm^{-1}). The light dispersed in this way was detected by a liquid-nitrogen-cooled CCD camera (operation temperature: –125 °C). The integration time of the CCD was set to 100 s. Three consecutive measurements of each sample were used for averaging and to reduce measurement uncertainties in the spectral acquisition process. To minimize possible photo degradation of the samples by UV radiation dissolved extracts and mushroom slices were placed on a rotating sample stage as displayed in Figure S4. The stage moved in a spiral path with a diameter of ~ 4 mm and a speed of 15 rpm. The data pre-processing and analysis was performed by in-house scripts in the programming language R.[9] Shortly, in a first step the wavenumber axes of the measured spectra were calibrated using a Teflon standard measured as a reference prior to the sample measurements. Subsequently spikes appearing due to cosmic radiation were removed. The background intensity was rejected by employing a statistic sensitive non-linear iterative peak-clipping algorithm (iterations = 100, algorithm order = 2, smoothing = false).[10] The background correction was supplemented by subtracting the averaged intensity between 1,940 and 2,040 cm^{-1} from each spectrum.

9.1. Sample preparation

White button mushrooms with a 3–5 cm diameter cap were bought from local supermarkets. The mushrooms were washed twice with cold water to remove dirt and cut into ~ 3 mm slices. Two mushroom slices were placed each in one part of the tripartite petri dish (Figure S13). The third part was filled with 500 µL of sterile H_2O. After inoculation of the mushroom slices with 20 µL of a *B. gladioli* pv. *agaricicola* overnight culture (PDB, 30 °C at 140 rpm, OD_{600} ~ 6.0) the petri dishes were incubated for 16 h at 30 °C. As controls the bacterial cell solution was replaced by either water or sterile overnight culture media.

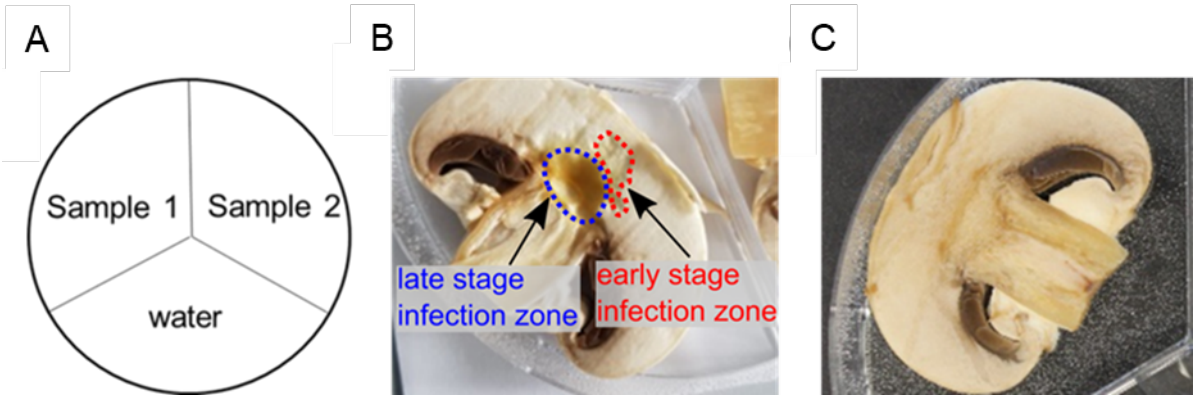

Figure S13. Sample preparation of infected mushrooms. A) Incubation of infected mushrooms in tripartite petri dishes. B) Slice of a white button mushroom inoculated with *B. gladioli* pv. *agaricicola* or C) water after incubation at 30 °C for 16 h. Lesions caused by the fungal pathogen can be seen in B) marked in blue. Smaller degradation of the mushroom tissue marked in red is visible in the area adjacent to the initially inoculated area marked in blue.

After incubation for 16 h at 30 °C, three different areas where distinguishable on the mushroom slices; first: non-infected tissue; second: strongly degraded, brown-yellowish tissue where the

mushroom was initially inoculated with the pathogenic bacteria. The latter is referred as “late-stage infection zone” in the following and marked in blue (Figure S13). The third region adjacent to the late-stage infection zone was only slightly degraded and is referred as “early-stage infection zone” in the following (marked in red, Figure S13).

9.2. Raman spectral data acquisition

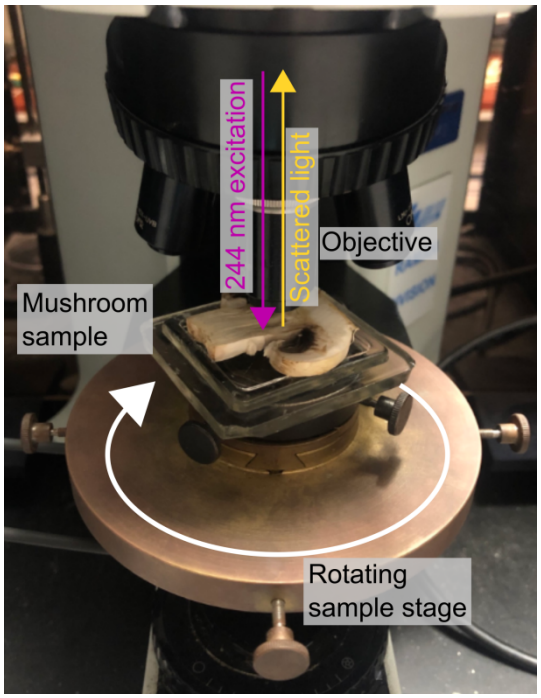

Figure S14. Display of the collecting optics of the UV Raman microspectroscopy setup with a rotating sample stage. To minimize possible photo degradation of the samples by UV radiation extracts and samples were placed on a rotating sample stage as displayed.

9.3. Spectral data processing

The data pre-processing and analysis was performed by in-house scripts written in the programming language R.[9, 11] Shortly, in a first step the measured spectra were wavenumber calibrated using a Teflon standard, measured as a reference prior to the sample measurements. Subsequently the spikes appearing in spectral channels were removed. The background intensity was rejected by employing a statistic sensitive non-linear iterative peak-clipping algorithm (SNIP).[12] Second-order algorithm with a clipping window of 100 was performed to generate an individual background, which was subtracted from the corresponding spectrum.

9.4. Density functional theoretic computation of Raman spectra

Density functional theory (DFT) calculations for the *cis*- and the *trans*-isoforms of caryoynencin (**7**) were performed utilizing the Gaussian 09 program package.[3] The calculations were performed using the B3LYP functional with the def2-TVZP polarized and diffuse triple-ζ basis set.[13] Geometry optimization was carried out, followed by a frequency analysis to confirm the relaxed geometry represents a minimum in the 3N-6-dimensional potential energy surface. Additionally, Raman activities were calculated for all vibrations which could then be used to

calculate a theoretical Raman spectrum. The Raman activities were converted to Raman intensities by employing the following equation:[13a]

$$R_i = \frac{(2\pi)^4}{45} \cdot (\nu_0 - \nu_i)^4 \cdot \frac{h}{8\pi^2 c\nu_i \left[1 - e^{-\frac{hc\nu_i}{kT}}\right]} \cdot S_i \qquad (1)$$

Herein R_i, S_i, ν_i, ν_0, h, c, T, k represent the Raman intensity, Raman activity, vibrational frequency of the ith band, frequency of the incident laser light (in this experiment 5.1688 × 10^{14} Hz or 244 nm), Planck's constant, the speed of light in vacuum, the temperature (in this case 298 K / 25 °C), and Boltzmann's constant. To account for the missing description of anharmonicity and electron correlation in the calculated frequencies, an empirical correction factor of 0.965 was employed. To visualize the spectra the calculated line spectrum was broadened using a Lorentzian function with a full-width-at-half-maximum of 18 cm^{-1}.[13b]

Figure S15 depicts the calculated Raman spectra of caryoynencin (**7**) for both *cis*- and the *trans*-isomers. In the following the *trans*-isomer was compared to measured extract and sliced mushroom samples.

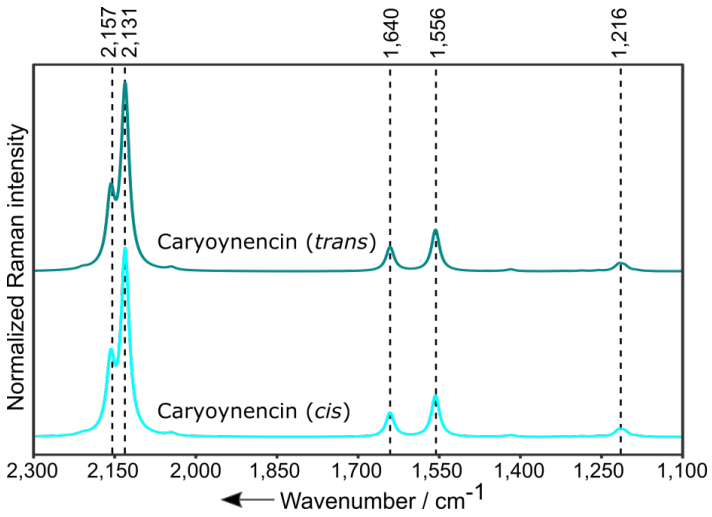

Figure S15. Wavenumber corrected, DFT-Calculated Raman spectra of the *cis*- and *trans*-isomers of caryoynencin (**7**) in the wavenumber region between 1,100 and 2,300 cm^{-1} (scaling factor: 0.965, FWHM: 18 cm^{-1}). The spectra are vector normalized and shifted vertically for better visualization.

9.5. Raman spectroscopic investigation of extract samples

Extracts of *B. gladioli* pv. *agaricicola* and mutant cultures were investigated by means of UV Raman spectroscopy. *B. gladioli* pv. *agaricicola* HKI0676 Δ*cay* and Δ*spg* is not able to produce **7** or **8**, respectively. Bacteria extracts were dissolved in methanol to a final concentration of 1 mg mL^{-1} ($m_{extract}$ / $V_{Methanol}$). The UV Raman measurements of dissolved extracts were conducted in a quartz cuvette under rotational movement to reduce photo degradation by UV radiation (see Raman spectral data acquisition).

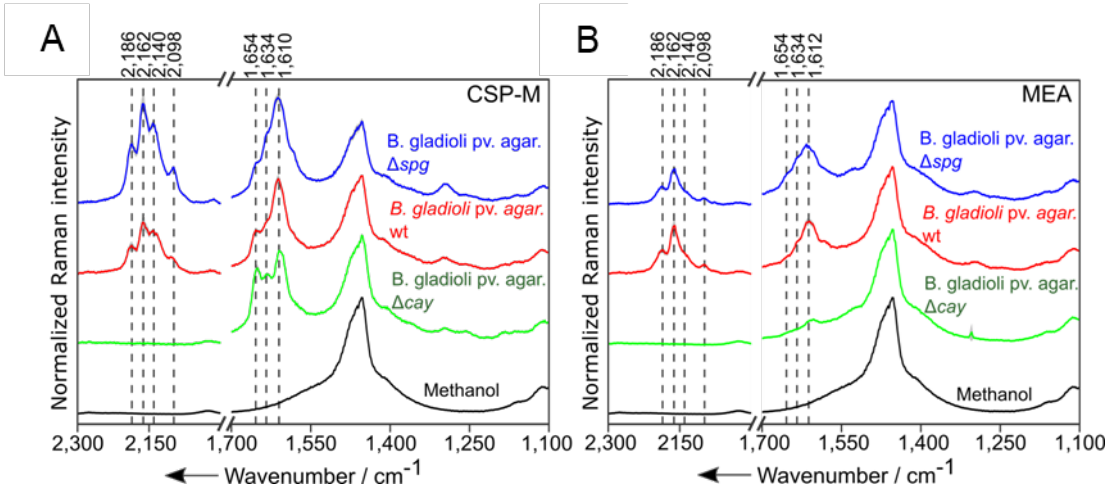

Figure **S16** shows the processed UV Raman spectra of the culture extracts (wild type and mutant extracts).

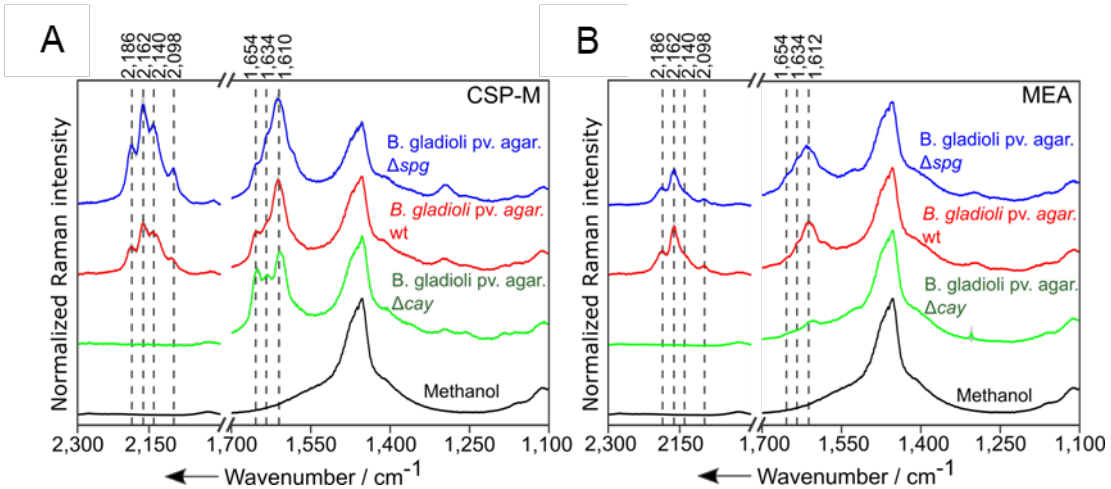

Figure S16. UV Raman spectra of dissolved bacterial extracts. A) Spectra of dissolved bacteria that produced **7** in CSP-medium and B) grown in MEA-medium that favors the production of **8** over **7**.

9.6. Comparison of spectra of infected mushroom tissue and DFT calculations

Figure S17 compares Raman spectra of infected mushroom tissue (blue), culture extract (brown) and a calculated spectrum of **7** in the wavenumber region between 2,050 and 2,250 cm^{-1}. The spectrum of the extract originates from the measurement of an extract of a *B. gladioli* pv. *agaricicola* wild type culture that was grown under conditions were caryoynencin (**7**) production occurs.

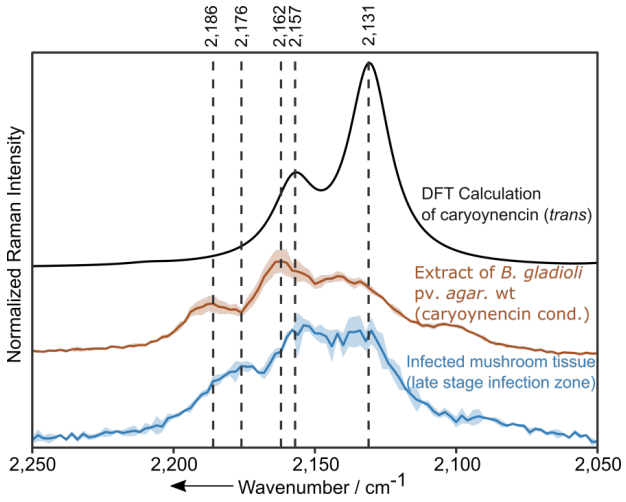

Figure S17. Zoom-in of measured and calculated Raman spectra. The standard deviations are show as shaded areas in the corresponding colors around each mean spectrum. All spectra are vector normalized and shifted vertically for better visualization.

9.7. Additional UV Raman measurements

Raman spectra supplementing the data shown in Figure 2e were recorded by means of UV Raman spectroscopy. Figure S18 displays additional measurements performed on mushroom slices: two infection zones (red/blue spectra) and mushroom slices where bacteria grown under conditions where no production of **7** occurs have been added shortly before the measurements.

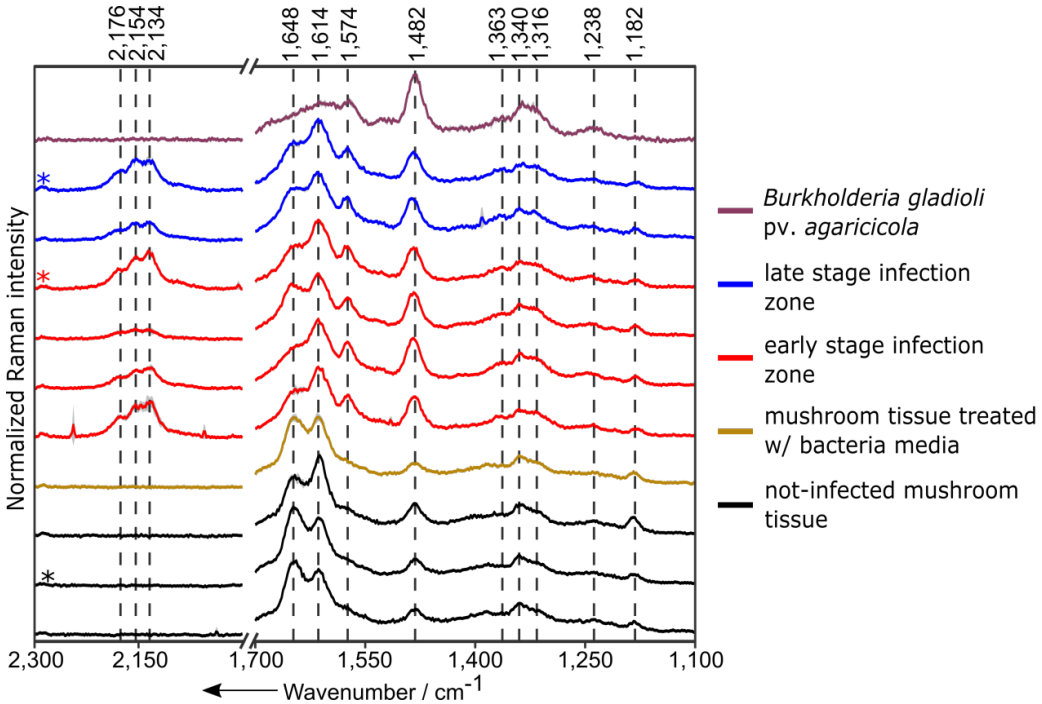

Figure S18. Additional UV Raman spectra of non-infected (black), infected (red/blue) mushroom tissues. A spectrum of a *B. gladioli* pv. *agaricicola* culture extract devoid of 7 and added shortly before the measurement on a mushroom tissue is depicted in purple. The spectra marked by an asterisk are presented partially in Figure 2e. The displayed spectra show the calculated average of three consecutive measurements. The standard deviations are shown as gray shaded areas around each mean spectrum. All spectra are vector normalized and shifted vertically for better visualization.

9.8. Frequency assignment

The most prominent peak in the spectrum of non-infect mushroom tissue is at 1,648 cm^{-1} and can be assigned to thymine's carbonyl band with contributions of proteins amid I vibration.[14] The peak at 1,614 cm^{-1} can be assigned to aromatic amino acids tryptophane and tyrosine.[10] The signal at 1,574 cm^{-1}, which was only visible as a shoulder in the Raman spectrum of the non-infected mushroom tissue, is more pronounced in the infection zones. Furthermore, the band intensities at 1482 cm^{-1} increase when measurements of infected to non-infected mushroom tissue are compared. Both peaks at 1,574 cm^{-1} and 1,482 cm^{-1} can be assigned to the nucleobases guanine and adenine.[10] The increasing guanine and adenine signals can be explained by the additional biomass due to bacteria on the mushroom tissue (see purple spectrum inFigure S18). The broad feature at ~ 1,340 cm^{-1} apparent in the infected/non-infected mushroom tissue, as well as in the bacteria spectra can be assigned to a superposition of several contributions from the biological matrix. The peak at 1,363 cm^{-1} is most likely associated with the ring breathing mode of tryptophane.[14a, 15] While the peak at 1,340 cm^{-1} can be assigned again to tryptophane and additionally to the nucleobases guanine and adenine.[10, 14a, 15-16] The latter nucleobases contribute furthermore to the shoulder feature visible in the Raman spectra at 1,316 cm^{-1}.[10, 14b] In the bacteria Raman spectrum the band at 1,238 cm^{-1} is very prominent and can be attributed to thymine. The latter band is particularly pronounced in the spectrum of the bacteria, only slightly apparent in the Raman spectra of the non-infected mushroom tissue and more discernible in the spectra of the investigated infected mushroom tissue. Again, the increase in band intensities in the spectra of the infected fungal tissue can be explained by the additional biomass of the bacteria on the mushroom tissue. The signal at 1,182 cm^{-1} present in the Raman spectra of both the infected and non-infected mushroom tissue can be assigned to tyrosine.[14a]

10. References

[1] T. Thongkongkaew, W. Ding, E. Bratovanov, E. Oueis, M. Garcia-Altares, N. Zaburannyi, K. Harmrolfs, Y. Zhang, K. Scherlach, R. Müller, C. Hertweck, *ACS Chem. Biol.* **2018**, *13*, 1370-1379.

[2] B. Dose, S. P. Niehs, K. Scherlach, L. V. Flórez, M. Kaltenpoth, C. Hertweck, *ACS Chem. Biol.* **2018**, *13*, 2414-2420.

[3] B. Gust, G. L. Challis, K. Fowler, T. Kieser, K. F. Chater, *Proc. Natl. Acad. Sci. U.S.A* **2003**, *100*, 1541-1546.

[4] B. Dose, S. P. Niehs, K. Scherlach, S. Shahda, L. V. Flórez, M. Kaltenpoth, C. Hertweck, *ChemBioChem* **2021**, *22*, 1920-1924.

[5] K. Ishida, T. Lincke, C. Hertweck, *Angew. Chem. Int. Ed.* **2012**, *51*, 5470-5474.

[6] J. Y. L. Y. S. Seo, J. Park, S. Kim, H. H. Lee, H. Cheong, S. M. Kim, J. S. Moon, I. Hwang, *BMC Genomics* **2015**, *16*, 349.

[7] a) L. V. Flórez, K. Scherlach, P. Gaube, C. Ross, E. Sitte, C. Hermes, A. Rodrigues, C. Hertweck, M. Kaltenpoth, *Nat. Commun.* **2017**, *8*, 15172; b) M. J. Beltran-Garcia, M. Estarron-Espinosa, T. Ogura, *J. Agric. Food Chem.* **1997**, *45*, 4049-4052.

[8] S. P. Niehs, J. Kumpfmüller, B. Dose, R. F. Little, K. Ishida, L. V. Florez, M. Kaltenpoth, C. Hertweck, *Angew. Chem. Int. Ed.* **2020**, *59*, 23122-23126.

[9] a) T. Bocklitz, A. Walter, K. Hartmann, P. Rösch, J. Popp, *Analytica Chimica Acta* **2011**, *704*, 47-56; b) T. W. Bocklitz, S. Guo, O. Ryabchykov, N. Vogler, J. Popp, *Anal. Chem.* **2016**, *88*, 133-151.

[10] Z. Q. Wen, G. J. Thomas, *Biopolymers* **1998**, *45*, 247-256.

[11] R. C. Team, *R: A Language and Environment for Statistical Computing*, Vienna, Austria, **2020**.

[12] C. G. Ryan, E. Clayton, W. L. Griffin, S. H. Sie, D. R. Cousens, *Nuclear Instruments and Methods in Physics Research Section B: Beam Interactions with Materials and Atoms* **1988**, *34*, 396-402.

[13] a) M. J. Frisch, G. W. Trucks, H. B. Schlegel, G. E. Scuseria, M. A. Robb, J. R. Cheeseman, G. Scalmani, V. Barone, G. A. Petersson, H. Nakatsuji, X. Li, M. Caricato, A. V. Marenich, J. Bloino, B. G. Janesko, R. Gomperts, B. Mennucci, H. P. Hratchian, J. V. Ortiz, A. F. Izmaylov, J. L. Sonnenberg, Williams, F. Ding, F. Lipparini, F. Egidi, J. Goings, B. Peng, A. Petrone, T. Henderson, D. Ranasinghe, V. G. Zakrzewski, J. Gao, N. Rega, G. Zheng, W. Liang, M. Hada, M. Ehara, K. Toyota, R. Fukuda, J. Hasegawa, M. Ishida, T. Nakajima, Y. Honda, O. Kitao, H. Nakai, T. Vreven, K. Throssell, J. A. Montgomery Jr, J. E. Peralta, F. Ogliaro, M. J. Bearpark, J. J. Heyd, E. N. Brothers, K. N. Kudin, V. N. Staroverov, T. A. Keith, R. Kobayashi, J. Normand, K. Raghavachari, A. P. Rendell, J. C. Burant, S. S. Iyengar, J. Tomasi, M. Cossi, J. M. Millam, M. Klene, C. Adamo, R. Cammi, J. W. Ochterski, R. L. Martin, K. Morokuma, O. Farkas, J. B. Foresman, D. J. Fox, *Gaussian 09 Rev. A.02*, Wallingford, CT, **2009**; b) F. Weigend, R. Ahlrichs, *Phys. Chem. Chem. Phys.* **2005**, *7*, 3297; c) A. Jevicki, C. Lee, *Phys. Rev. D* **1988**, *37*, 1485-1491.

[14] a) S. P. A. Fodor, R. A. Copeland, C. A. Grygon, T. G. Spiro, *J. Am. Chem. Soc.* **1989**, *111*, 5509-5518; b) R. M. Jarvis, R. Goodacre, *FEMS Microbiol. Lett.* **2004**, *232*, 127-132.

[15] N. Tarcea, M. Harz, P. Rösch, T. Frosch, M. Schmitt, H. Thiele, R. Hochleitner, J. Popp, *Spectrochimica Acta Part A: Molecular and Biomolecular Spectroscopy* **2007**, *68*, 1029-1035.

[16] M. Harz, R. A. Claus, C. L. Bockmeyer, M. Baum, P. Rösch, K. Kentouche, H. P. Deigner, J. Popp, *Biopolymers* **2006**, *82*, 317-324.